



Enhancement of proton conduction in carboxymethyl cellulose-polyvinyl alcohol employing polyethylene glycol as a plasticizer

M A SAADIAH^{1,2}, H M TAN² and A S SAMSUDIN^{2,*} 

¹Department of Chemistry, Centre for Foundation Studies, International Islamic University Malaysia, 26300 Gambang, Pahang, Malaysia

²Ionic Materials Team, Faculty of Industrial Sciences and Technology, Universiti Malaysia Pahang, 26300 Kuantan, Pahang, Malaysia

*Author for correspondence (ahmadsalihin@ump.edu.my)

MS received 23 August 2019; accepted 20 March 2020; published online 12 August 2020

Abstract. The present study deals with the enhancement of proton transport and conduction properties of solid polymer electrolyte (SPE)-based carboxymethyl cellulose (CMC) blended with polyvinyl alcohol (PVA) doped with ammonium nitrate (NH_4NO_3) and plasticized with various compositions of polyethylene glycol (PEG). The SPE system was successfully prepared using an economical method, the solution casting technique, and analysed by Fourier transform infrared spectroscopy and electrical impedance spectroscopy. The infrared spectra show that interaction had occurred at O–H and COO^- from CMC when PEG was added which prevailed the enhancement of ion dissociation. Glass transition measurement highlighted that the interaction between CMC–PVA– NH_4NO_3 and ethylene carbonate at 8 wt% give the most plasticization effect that achieved the lowest T_g . The highest conductivity of the SPE system achieved at ambient temperature was $1.70 \times 10^{-3} \text{ S cm}^{-1}$ for a non-plasticized sample, and further enhanced to $3.00 \times 10^{-3} \text{ S cm}^{-1}$ when 8 wt% PEG was incorporated into the SPE system. The sample with the highest conductivity was found to obey the Arrhenius behaviour with a function of temperature. The ionic conductivity of the SPE system was shown to be primarily influenced by a number of ions (η), ion mobility (μ) and diffusion coefficient (D).

Keywords. CMC–PVA– NH_4NO_3 ; PEG; ionic transport.

1. Introduction

Conventional lithium-ion liquid electrolyte batteries have gained an unforeseen importance in the last few decades in portable electronic devices such as laptop computers, mobile phones and electric cars [1]. Alkaline batteries were being produced more than 10 billion units per year and a majority of these batteries end up at landfills [2]. However, liquid electrolyte batteries are an inherent hazard to leakages and explosions. Due to continuous charging of liquid electrolyte batteries, it will lead to loss of battery quality. Hence, all these factors have contributed to the development of solid polymer electrolytes (SPEs) [1,3,4]. Moreover, due to the rapid growth in microelectronics circuits, demand for lightweight batteries with high energy density and high cycle life is increasing rapidly. In the application of SPEs, some improvisation is needed to increase the ionic conductivity. A comprehensive study is required to focus on the substitute of liquid electrolytes which was commercially used in energy storage. The new substitute should use safer materials which certainly contribute to the sustainability of the environment. Hence, the advent of SPEs based on bio-

resources has been researched and developed to disclose possible alternatives with much superior properties, non-hazardous properties and good biocompatibility [5].

Notwithstanding four decades of attempts, the potential of SPEs as hosts for great ionic mobility has not been realized. To date, lots of studies have been carried out to improve SPE properties including the use of copolymers and addition of dopants or plasticizers [6]. In SPEs, composition of salt or plasticizer affects the ionic conductivity. Among the pioneering studies in the field of SPEs, the combination of polyethylene glycol (PEG) and lithium perchlorate (LiClO_4) had achieved a maximum conductivity of $7.3 \times 10^{-7} \text{ S cm}^{-1}$ [7]. Parameswaran *et al* [8] observed an electrical conductivity for a zwitterionic polymer blend incorporated with ammonium bromide which was enhanced to $\sim 10^{-4} \text{ S cm}^{-1}$ for battery application. Similarly, Aziz [9] investigated SPEs based on polycaprolactone with lithium bis(oxalato)borate as a doping salt. The result revealed that DC electrical conductivity and dielectric constant of SPEs had increased with concentration of salt up to 4 wt%. Several studies have reported based on carboxymethyl cellulose (CMC)–polyvinyl alcohol (PVA)

incorporated with different ionic dopants including NH_4Cl [10], NH_4Br [11] and NH_4NO_3 [12] with a conductivity in the range of $\sim 10^{-5}$ to 10^{-3} S cm^{-1} , respectively. Hence, most of the studies have been focusing on alternatives to overcome the limitations of SPE systems in terms of enhancement of mobility-limiting polymer chains which might affect the conductivity of SPEs.

The incorporation of plasticizers provides new pathways for the dissociation of the salt by weakening the force between the cations and anions and causes the salt to dissociate more easily into free ions [13]. This pathway could be attributed to the significant changes in the local structure by complexation which leads to increment in the amorphous region, decrement of glass transition temperature and eventually enhanced the ionic conductivity [14]. A number of authors have considered the effect of addition of plasticizers which is regarded as the most effective way to improve the ionic conductivity [15]. Therefore, this encouraged many researchers to assess the effect of various plasticizers such as ethylene carbonate (EC) [16], glycerol [17], dimethylacetamide [18] and tetra(ethylene glycol)dimethyl ether [19]. In the same vein, Ng and Mohamad [20] studied proton batteries based on chitosan SPEs incorporated with NH_4NO_3 and EC as plasticizers in acetic acid solution and succeeded in enhancement of the conductivity from $\sim 10^{-5}$ to $\sim 10^{-3}$ S cm^{-1} . In this present study, PEG was added into polymer complexes CMC–PVA– NH_4NO_3 because a limited number of research studies have used PEG as a plasticizer thus far. Herein, the present study has used CMC–PVA– NH_4NO_3 which was optimized at 56:14:30 due to the favourable conduction as reported in a previous preliminary study [12] as a polymer electrolyte system and plasticized with PEG. This is an attempt to evaluate the effectiveness of PEG as a plasticizer for the CMC–PVA incorporated with NH_4NO_3 . To understand how various compositions of PEG affects the complexation and ionic transport properties, simple approaches e.g., Fourier transform infrared (FTIR), differential scanning calorimetry (DSC) and electrical impedance spectroscopy (EIS) were used in characterization. Furthermore, the deconvolution technique was adopted and parameters including number of mobile ions, ionic mobility and diffusion coefficient were compared systematically based on various PEG compositions. To the best of author's knowledge, none of the previous literature reports has investigated the proton conduction enhancement of CMC–PVA– NH_4NO_3 influenced by PEG which could enlighten this newly developed SPE as a promising electrolyte in various applications.

2. Experimental

2.1 Preparation of SPE sample

CMC (Acros Organics, M.W. 90,000) and partially hydrolysed PVA (Merck Schuchardt OHG, M.W. 70,000) with an 80:20 composition of 2.00 g were dissolved in

distilled water at room temperature prior to the addition of 30 wt% equivalent of 0.857 g of NH_4NO_3 (Merck KGaA, $M = 80.04$ g mol^{-1}) [12]. The mixed solution was stirred continuously until complete dissolution was achieved. Various weight percents of PEG (Sigma Aldrich, $M_n = 1,100$) were incorporated into the doped polymer blend and stirred homogeneously. The indication of sample compositions is tabulated in table 1. The mixtures were casted into Petri dishes and dried using an oven for about 5 h at 60°C .

2.2 Characterization of CMC/PVA SPEs

2.2a FTIR spectroscopy: A Spectrum One (Perkin Elmer, USA) FTIR spectrometer equipped with zinc selenium (ZnSe) attenuated total reflectance (ATR) was used to analyse the complexation of polymer–proton interactions, the formation of ternary blends and the surface composition of samples. The frequency range was set from 4,000 to 700 cm^{-1} with a total of 10 scans at a resolution of 2 cm^{-1} .

2.2b DSC: The thermal study was carried out using a DSC 214 Polyma (Netzsch, Germany) where ~ 3.00 mg of sample was weighed into an aluminium pan. The sample was heated up to 400°C at a heating rate of $10^\circ\text{C min}^{-1}$ and purged under a nitrogen flow at a rate of 40 ml min^{-1} .

2.2c EIS: SPE samples were characterized using EIS with a HIOKI 3532-50 LCR Hi-Tester interfaced to a computer in the frequency range between 50 Hz and 1 MHz. The samples were cut into suitable size and placed in between the electrodes. From the plot of imaginary part (Z_i) vs. real part (Z_r) of impedance, the bulk resistance R_b of SPE films could be determined. The ionic conductivity, σ , can be calculated using the following equation:

$$\sigma = \frac{l}{R_b A}, \quad (1)$$

where l is the thickness of the film and A is the electrode–electrolyte contact area in the SPE films in cm^2 . The thickness of the SPEs was measured using a digital thickness gauge (DML3032).

Table 1. List of samples with their compositions.

Indication	Composition of PEG (wt%)
C0	0
C2	2
C4	4
C6	6
C8	8
C10	10
C12	12

2.2d FTIR deconvolution: The deconvolution method was carried out using Origin Pro (by Gaussian–Lorentz function) to determine the number of ions (η), mobility of ions (μ) and diffusion coefficient (D). The baseline function was utilized to deconvolute a specific region and analysed transport properties. In this method, the FTIR peaks attributable to the dominant ionic movement were studied and the total intensity of all the deconvoluted peaks was determined to fit the original spectrum [21]. The area under the peaks was deduced and the percentage of free ions was calculated using the following equation [22]:

$$\text{Percentage of free ions (\%)} = \left(\frac{A_f}{A_f + A_c} \right) \times 100\%, \quad (2)$$

where A_f is the area under the peak indicating the free ion region, A_c is the sum of area under the peak indicating the contact ions, M is the moles of each wt% PEG, N_A is the Avogadro's constant, V_{total} is the total volume of the SPE system, k is the Boltzmann constant, T is the absolute temperature and e is the electron charge. The number of density (η), diffusion coefficient (D) and mobility (μ) of the ions were calculated using the following equations [21,23–25]:

$$\eta = \left(\frac{M \times N_A}{V_{\text{total}}} \right) \times \text{free ions (\%)}, \quad (3)$$

$$\mu = \left(\frac{\sigma}{\eta e} \right), \quad (4)$$

$$D = \left(\frac{kT\mu}{e} \right). \quad (5)$$

3. Results and discussion

3.1 ATR-FTIR analysis

Figure 1 shows the IR spectra of three important regions which correspond to the presence of asymmetrical COO^- , bending $-\text{OH}$ and stretching $-\text{OH}$ which are crucial functional groups to the interaction of coordination in CMC–PVA– NH_4NO_3 and PEG. The changes in wavenumber for the complexation taken place in SPEs are tabulated in table 2. Figure 1a depicts the IR spectra of the CMC–PVA– NH_4NO_3 –PEG SPE system at $1,312 \text{ cm}^{-1}$ which agrees with the presence of $-\text{OH}$ (hydroxyl) bending. Based on the figure, it is evident that the hydroxyl band has shifted to higher wavenumber $1,333 \text{ cm}^{-1}$ as the amount of PEG increased. This phenomenon implied that the PEG promotes the occurrence of H-bonding in the SPEs [26,27]. Moreover, the band became wider due to the formation of rather strong hydrogen bonds between the O–H and $\text{NH}_3\text{--H}^+$ [28].

On contrary, it can be observed in figure 1b that the intensity of the peak at $1,579 \text{ cm}^{-1}$ was discovered to reduce with the addition of PEG. The changes are

considered due to the coordination interaction of $-\text{COO}^-$ in CMC with H^+ of $[\text{NH}_4^+]$ substructure in NH_4NO_3 which reveals that the higher the PEG composition, the higher the number of H^+ withdrawn towards the $-\text{COO}^-$. The shifting towards higher wavenumber infers that complexation has taken place between the CMC–PVA– NH_4NO_3 and PEG which was due to the formation of intra-molecular H-bonding attraction [29]. This interaction also allowed the protonation and deprotonation to occur from one $-\text{COO}^-$ to another $-\text{COO}^-$ by ion hopping. PEG is regarded as a representative that could shorten the distance of the ion-hopping mechanism by providing a new alternative pathway [30]. In addition, the appearance of small hump at $1,710 \text{ cm}^{-1}$ in the adjacent position of $-\text{COO}^-$ becomes more apparent after the addition of PEG which suggests the success of the plasticization.

Figure 1c evidences that the complexation leads to a shift in a wide contour absorption band of CMC–PVA, that is, the stretching $-\text{OH}$ group is located in the $2,800\text{--}3,800 \text{ cm}^{-1}$ region. Indeed, more hydrogen bonds have formed due to the increment of PEG composition which was shown by the plateau in that region [31,32]. This could explain that the addition of a plasticizer caused the growth in the number of free ions which encourage more complexation to occur [13].

3.2 Thermal analysis

DSC has been performed to determine the glass transition temperature (T_g) upon the incorporation of PEG into the CMC–PVA– NH_4NO_3 . The DSC thermogram for various samples of CMC–PVA– NH_4NO_3 –PEG is depicted in figure 2.

The determination of T_g was performed at the midpoint of the endothermic peak and shown as an inset in figure 2. Based on the data, the addition of PEG has reduced the T_g value. This pattern could be deduced as a result of reduction in segmental motion which was ascribed to the coordination interaction of $-\text{COO}^-$ in CMC with H^+ of $[\text{NH}_4^+]$ substructure in NH_4NO_3 explained by FTIR previously. Notably, the plasticization effect contributed by PEG has weakened the Columbic forces (dipole–dipole and hydrogen bonding) of the host polymer and NH_4NO_3 which in turn create a transient or temporary bonding during the interaction between the CMC–PVA– NH_4NO_3 and PEG [33]. Consequently, the energy barrier for the protonation and migration of H^+ could be reduced. This is aligned with the result of present study, where a reduction of T_g from 88.65 to 48.99°C was observed with the addition of PEG up to 8 wt%. The decrement of T_g may be attributed to the plasticization effect (polymer–salt complex softening) by the PEG and it causes the polymer chain to become more flexible [34]. This observation is in good agreement with the result reported by Greco *et al* [35], who investigated the T_g dependency to be due to the miscibility of the plasticized

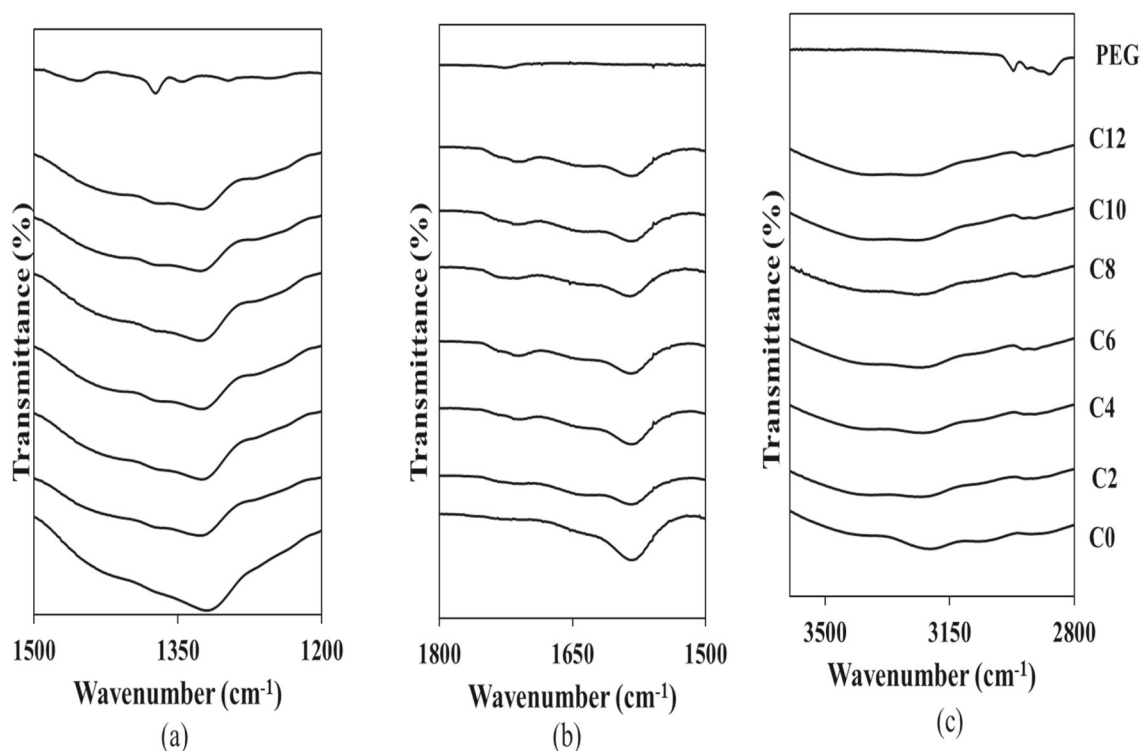


Figure 1. FTIR spectra of the CMC–PVA–NH₄NO₃–PEG SPE system of (a) 1,200–1,500 cm⁻¹, (b) 1,500–1,800 cm⁻¹ and (c) 2,800–3,800 cm⁻¹.

Table 2. List of important FTIR vibrational modes of SPEs.

Sample	Vibrational modes (cm ⁻¹)		
	Bending –OH	Asymmetrical –COO ⁻	Stretching –OH
C0	1,312	1,579	3,381
C2	1,318	1,578	3,377
C4	1,320	1,579	3,376
C6	1,324	1,581	3,375
C8	1,325	1,583	3,368
C10	1,330	1,586	3,365
C12	1,333	1,587	3,361

system. Similarly, Ahmadi-Khaneghah *et al* [36] found that the polyethylene segment in the PEG managed to decrease the T_g and resulted in the increase of chain mobility. Thus, the addition of PEG causes the SPE to behave as a rubber-like material at lower temperature. Additionally, the presence of PEG in the SPE leads to good compatibility and resulting in a miscible system. This could be evidenced by the occurrence of single glass transition which was observed for all samples.

Together, the effect of incorporation of PEG into the SPE towards the glass transition temperature was compared with previous studies and tabulated in table 3. A recent study by

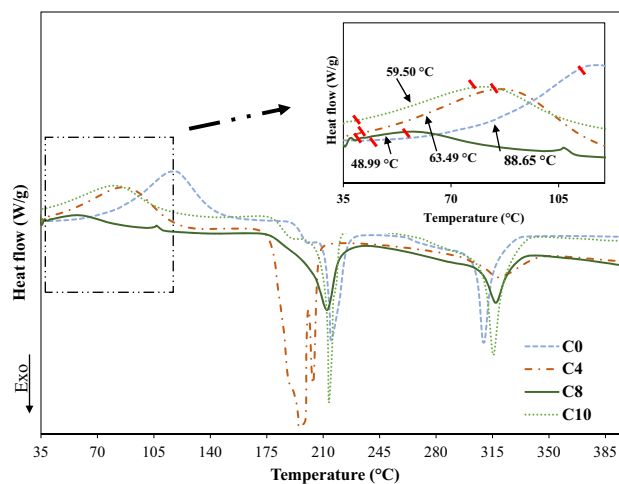


Figure 2. DSC thermogram of CMC–PVA–NH₄NO₃–PEG (inset: glass transition temperature of the CMC–PVA–NH₄NO₃–PEG SPE system).

Devangamath *et al* [37] involved a comprehensive research on the glass transition temperatures of pure PVA and PEG in which the value was obtained as 85 and 63°C, respectively. In this present study, PEG was added to the CMC–PVA–NH₄NO₃ to weaken the Coulombic force in the NH₄NO₃ which facilitate the modification of a three-dimensional molecular arrangement of the SPEs, thereby reducing the energy required for the phase transition to occur [38]. Consistent with the literature, the T_g achieved by

Table 3. Comparison of glass transition temperature of the present SPEs and other systems.

SPE	Glass phase transition, T_g (°C)	Reference
Cellulose–ECH–PEG	183	[40]
PVA–PEG	95	[37]
PVA–PVP–PEG	64.13	[41]
CMC–PVA– NH ₄ NO ₃ –PEG	48.99	Present study

ECH, epichlorohydrin; PVP, polyvinylpyrrolidone.

present SPEs based on CMC–PVA–NH₄NO₃–PEG exhibited a lower value than that of other SPE systems listed in the table suggesting the success of plasticization effect. Aziz *et al* [39] performed a conceptual review of the ion transport in the polymer electrolyte and confirmed that the three-dimensional molecular arrangement of the SPE could lead to an increase in the free volume of the system, which

can boost the movement of ionic charge carriers, H⁺. This successively would favour the enhancement of ionic conductivity in the SPEs.

3.3 Ionic conductivity analysis

The ionic conductivity of the CMC–PVA–NH₄NO₃–PEG SPE system at ambient temperature is depicted in figure 3. Based on a previous report [42], the highest conductivity for the CMC–PVA–NH₄NO₃ SPE system was stated at $1.70 \times 10^{-3} \pm 6.01 \times 10^{-4} \text{ S cm}^{-1}$ for the sample containing 30 wt% NH₄NO₃. In the present system, the ionic conductivity further increased to $3.00 \times 10^{-3} \pm 8.76 \times 10^{-4} \text{ S cm}^{-1}$ when 8 wt% of PEG was added to the SPE system. Based on the figure, the amount of 8 wt% PEG is adequate to aid in the dissociation of H⁺ from NH₄NO₃. However, a minimal increment in ionic conductivity was observed and raised an intriguing question regarding the factors governing the enhancement of ionic conductivity. Drawing on

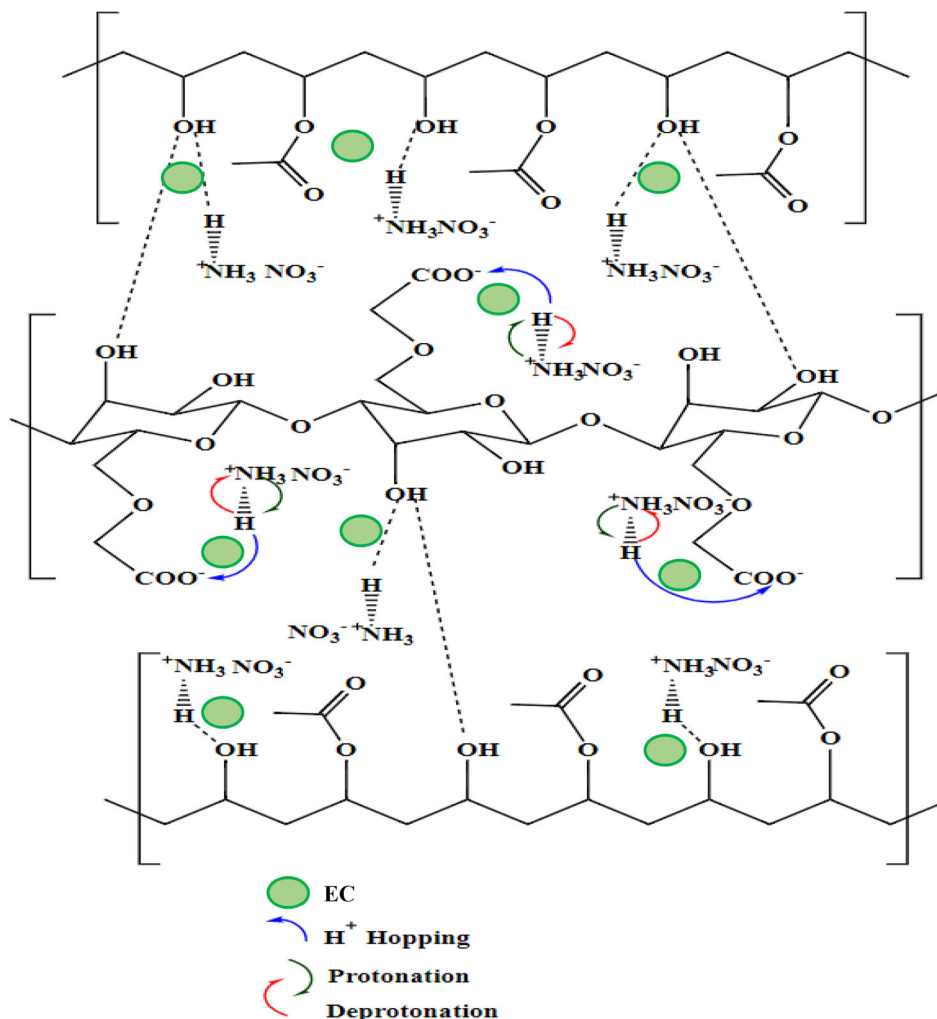
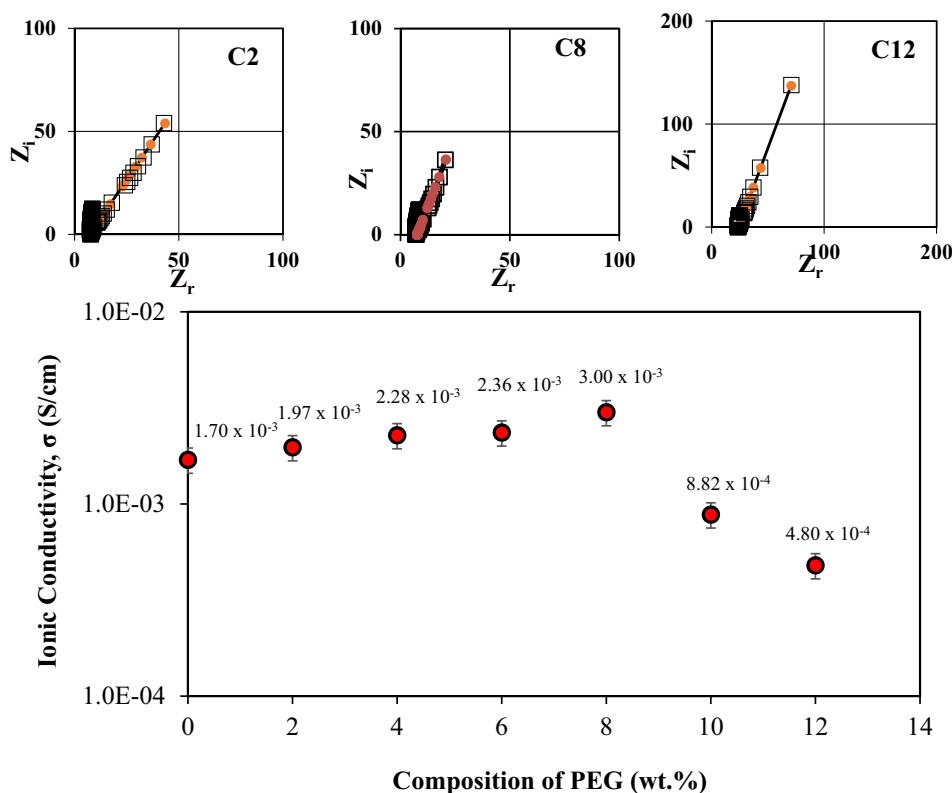
**Figure 3.** Schematic diagram of the reaction mechanism for the plasticization effect on the CMC–PVA–NH₄NO₃–PEG SPE system.

Table 4. Comparison of un-plasticized and plasticized ionic conductivity of the present SPEs and other systems.

SPE	Ionic conductivity ($S\text{ cm}^{-1}$)	Reference
CH–MC–LiBr ₄	3.74×10^{-6}	[49]
CH–MC–LiBr ₄ –PEG	2.12×10^{-5}	
Agar–agar–NH ₄ Br	7.24×10^{-5}	[50]
Agar–agar–NH ₄ Br–EC	3.73×10^{-4}	
2-HEC–NH ₄ NO ₃	4.51×10^{-4}	[44]
2-HEC–NH ₄ NO ₃ –EC	1.17×10^{-3}	
PVP–MSA	1.16×10^{-5}	[45]
PVP–MSA–DMC	3.27×10^{-5}	
PEO–PAM–NaCF ₃ SO ₃	8.32×10^{-6}	[47]
PEO–PAM–NaCF ₃ SO ₃ –EC + PC	5.74×10^{-4}	
CMC–PVA–NH ₄ NO ₃	1.70×10^{-3}	Present study
CMC–PVA–NH ₄ NO ₃ –PEG	3.00×10^{-3}	

PEO, polyethylene oxide; PAM, polyacrylamide; PVP, polyvinylpyrrolidone; MSA, methanesulphonic acid; MC, methyl cellulose; NH₄CF₃SO₃, ammonium trifluoromethanesulphonate; EC, ethylene carbonate; Gly, glycerol; LiOAc, lithium acetate; DMC, dimethyl carbonate.

**Figure 4.** Ionic conductivity of various PEG wt% at room temperature and Cole–Cole plot of C2, C8 and C12 SPE systems.

extensive factors affecting the ionic conductivity, three important aspects could be highlighted from the present study which include lower dielectric constant properties of the plasticizer, suppression in ion dissociation and number of free ions (H^+) dissociated from NH_4^+ . Despite the fact of slight increase in the ionic conductivity value, this finding could contribute to decipher the function of the plasticizer in polymer–salt complexes. Muhammad *et al* [43] also point

out that the ionic conductivity was attributed to a dielectric constant of the plasticizer which resulted in greater ion dissociation and hence higher ionic conductivity. Another observation was reported by Hafiza and Isa [44] and Ambika *et al* [45] where the addition of a plasticizer in polymer salt complexes has increased the ionic conductivity only slightly which shows a similar trend to the present study. In addition, it is encouraging to compare this result

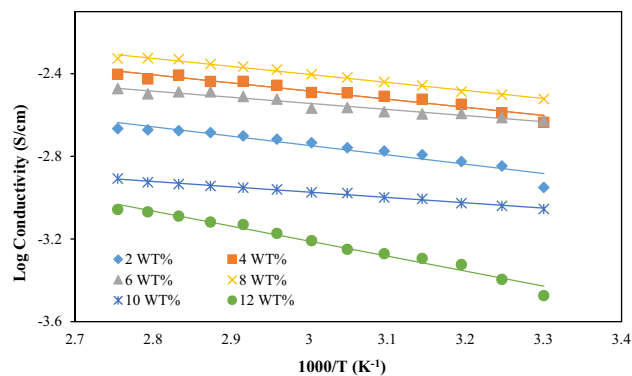


Figure 5. Temperature dependence of ionic conductivity for the CMC-PVA-NH₄NO₃-PEG SPE system.

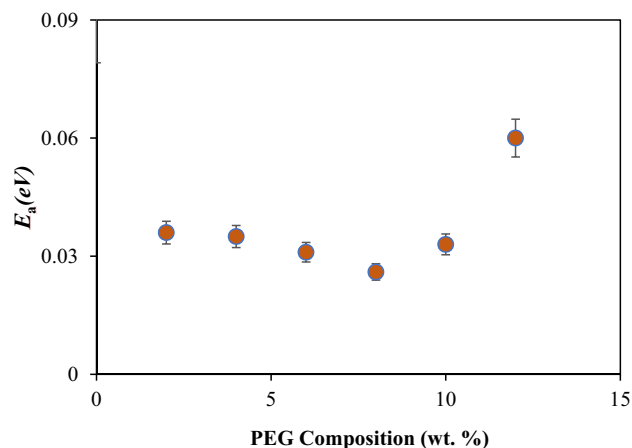


Figure 6. Activation energy E_a for various SPE systems.

with that of Das and Ghosh [46] who found that the enhancement in ionic conductivity was mainly influenced by the dielectric value of the plasticizer. The observed increase in ionic conductivity could be attributed to the lower dielectric constant value of PEG ($\epsilon_r = 12.4$) compared to other plasticizers [44]. Therefore, Dave *et al* [47] have attempted to investigate the combined effect of two plasticizers (EC + PC) to boost the ionic conductivity of polymer-blend systems.

Nevertheless, in contrast this finding could give significant implications for the understanding of the enhancement of ionic conductivity by increment of PEG composition based on the capability of PEG to enhance the dissociation of un-dissociated or salt aggregation towards the production of more free hydrogen conducting ions. This can be verified in terms of increase in the non-bridging ions between the hydroxyl group from PEG and hydrogen conducting ions from NH₄NO₃. This allows the released H⁺ to migrate towards the COO⁻ group of CMC. As the amount of PEG increases, the number of transit sites for the H⁺ ions increase considerably. This inspection was confirmed by FTIR analysis whereby the addition of PEG provides

alternative pathways for the protonation of hydrogen ions as depicted in figure 3.

In addition, the improvement in the ionic conductivity of the SPE system is because PEG provides a large free volume of relatively significant conducting phase and it also provides good thermal stability that would open channels for greater ionic transport [48]. The plasticizer provides free volume that exists between the biopolymer chains and allows a massive amount of H⁺ ions to move without any restriction. Apparently, PEG does not supply ions towards the SPE system, but it is believed that PEG aided in dissociation of NH₄NO₃ in the CMC-PVA matrix. This is due to the weakening of the inter-ion Coulomb force between the cations and anions in NH₄NO₃ causing the increase in hydrogen conducting ions (H⁺) with an increase in plasticization [48]. However, it shows that beyond 8 wt% of the CMC-PVA-NH₄NO₃-PEG SPE system, the conductivity decreases, and this might be caused by the re-association of ions. Table 4 provides a comparison of ionic conductivity for the polymer-salt complex systems incorporated with various types of plasticizers. The finding reveals that the present system based on CMC-PVA-NH₄NO₃ added with PEG as a plasticizer achieved relatively higher ionic conductivity compared to other plasticized SPE systems. This indicates that the combination of CMC-PVA-NH₄NO₃ and PEG may possibly provide a better pathway for the ion conduction mechanism and resulting in higher ionic conductivity.

The Cole-Cole plot of the selected CMC-PVA biopolymer blend doped with NH₄NO₃ and further plasticized with 2, 8 and 12 wt% of PEG is also presented in figure 4. The Cole-Cole plot revealed the occurrence of a spike line which may be caused by the ion migration occurred in the matrix polymer [51]. The spike line is determined by the influence of electrode polarization. Moreover, it shows that the total conductivity is principally the outcome of the ion conduction of the SPE system and the current carriers are ions [52,53]. The increment of the spike was considerably moving towards the higher range of frequency and the inclination of the spike was <90° with the real axis due to rapid relaxation of the dipolar in the CMC-PVA-NH₄NO₃-PEG system after the addition of 8 wt% (C8), which could have enhanced the conductive properties [24,54].

Figure 5 illustrates the temperature dependence of ionic conductivity for the SPE system studied in the temperature range of 303–363 K. This is to study the temperature-conductivity behaviour of the SPE system plasticized with PEG. Based on the figure, the increment in temperature causes an increase in conductivity and it is clearly shown that the graph of log conductivity vs. $1,000/T$ is linear which indicate that the temperature dependent ionic conductivity obeyed the Arrhenius relationship using the following equation:

$$\sigma = \sigma_0 \exp(-E_a/kT), \quad (6)$$

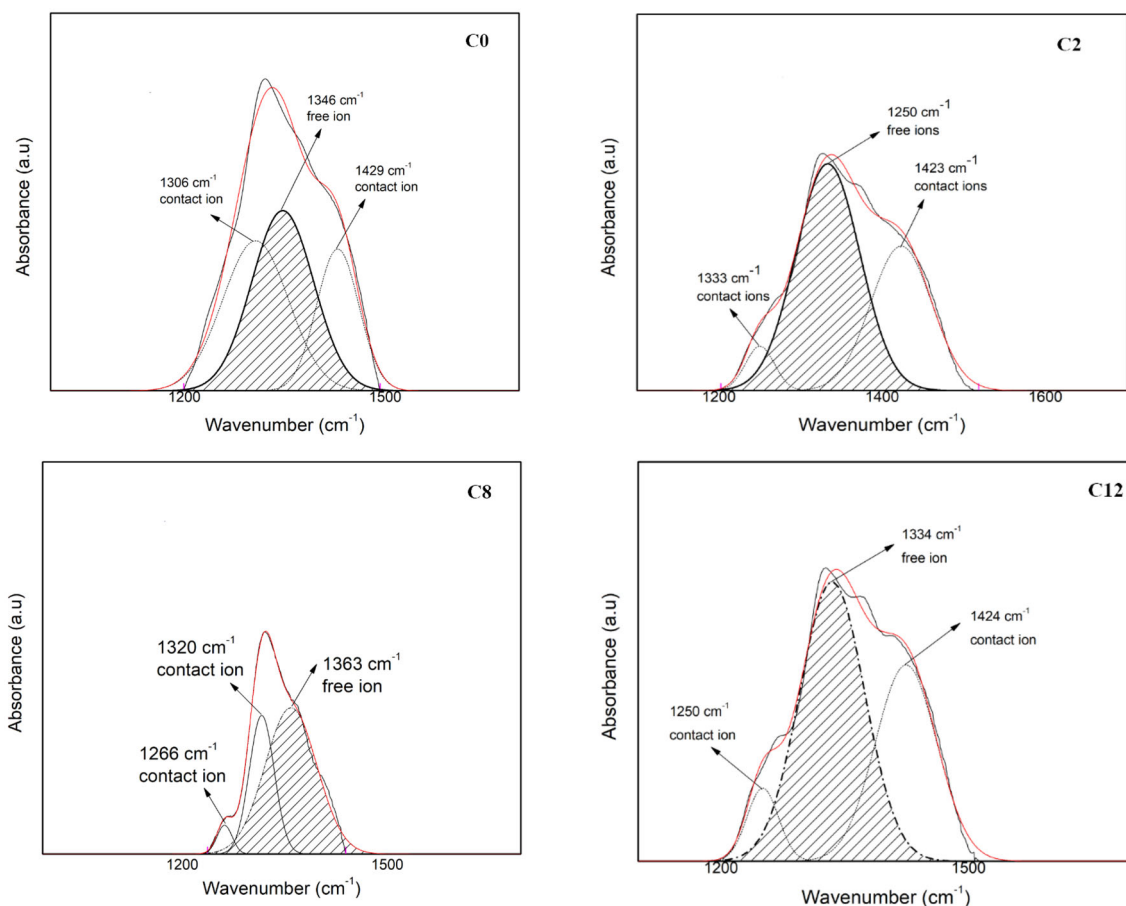


Figure 7. Deconvolution IR spectrum for the selected sample of the SPE system.

Table 5. Contact and free ions of the CMC–PVA–NH₄NO₃–PEG SPE system.

Samples	Free ions (%)	Contact ions (%)
C0	42.08	57.92
C2	47.72	52.28
C4	52.62	47.38
C6	62.91	37.09
C8	70.61	29.39
C10	60.32	39.68
C12	59.05	40.95

where σ_0 is the pre-exponential factor, k is the Boltzmann constant, T is the absolute temperature and E_a is the activation energy.

As temperature increases, the dissociation of salts, thermal movement of biopolymer chain segments and amorphousness of the SPE system also increase gradually. This demonstrates that the SPE system is thermally assisted. The extension of this study is the determination of activation energy, E_a . Figure 6 shows the value of E_a for various compositions of PEG which decreases gradually as the

conductivity of SPE samples increases until the addition of 8 wt% of PEG. This observed result corresponds to an increase in the number of mobile ions in the SPE system. As the greater amount of PEG particles had been ionized in the salt polymer complexes, the more prominent is the structural disorderliness that enhances the flexibility of the CMC backbone. This will further enhance the migration of hydrogen mobile ions [55–57]. However, the value has increased beyond the addition of 8 wt% of PEG which might be due to the overcrowded of ion aggregation. It is observed that the sample with the lowest E_a would have the highest ionic conductivity. The E_a of 8 wt% PEG composition is the lowest which is 0.026 eV. Because the E_a of this SPE system is considerably low, it is significant for practical applications in electrochemical devices and storage.

3.4 Ionic transport analysis

As discussed based on FTIR, the –OH bending located in the 1,200–1,500 cm⁻¹ region has exerted a stronger H-bonding. Thus, to further identify the hydroxyl band, deconvolution was performed for the selected SPEs as shown in figure 7. Based on the figure, the free ion represents the free mobile ions which are more likely H⁺ ions

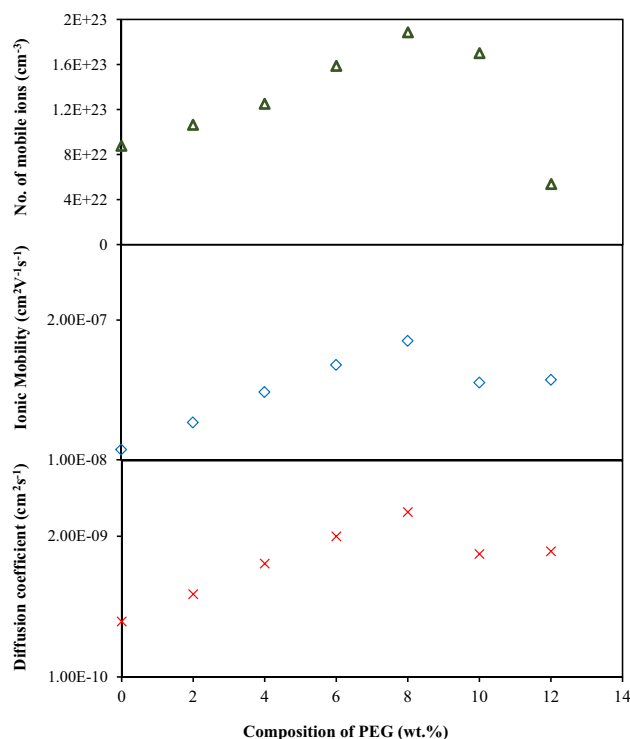


Figure 8. Transport parameters of various compositions of SPE system for number of mobile ions, η ; mobility, μ and diffusion coefficient, D .

and the contact ion pairs represent the contact ions including NH_4^+ and NH_3^- [58]. The contact and free ions were calculated from the percentage of the area of contact or free ions in the entire area of deconvolution peaks, respectively which are tabulated in table 5. The percentage of free ions with an increment of PEG composition until C8 can be observed. This is due to an upsurge of dissociation of H^+ ions from NH_4^+ which would lead to an increase in ionic conductivity. The highest ionic conductivity was achieved due to the formation of greatest number of free ions. This result facilitates the ionic conductivity remark in the SPE system.

It can be observed that the ratio of free ions has increased when the PEG composition is added until 8 wt% which has assisted the ion dissociation of H^+ ions from the salt. Notably, the ionic conductivity has improved as observed from the analysis of ionic conductivity discussed previously. However, at 10 and 12 wt%, the percentage of free ions decreases drastically due to the formation of ion aggregates that reduced the ionic conductivity. Based on table 5, it is observed that the current system becomes more capacitive than resistive as PEG increases until the optimum value is achieved for sample C8. The increment in the capacitance value with the increase of PEG content shows that the SPE system is suitable for the application in electrochemical devices [21,49].

Based on the information of free and contact ions, the number of ionic mobility (μ), mobile ions (η) and diffusion

coefficient (D) were calculated using equations (3, 4 and 5) and are presented in figure 8. Based on figure 8, it can be noted that the values of η , μ and D increased with increasing EC composition until sample C8 and reduced at higher PEG composition. This behaviour follows the trend of conductivity–composition of EC as depicted in figure 8 and found to be similar to transport properties from other research studies [59–62]. In the present system, the addition of PEG into CMC–PVA– NH_4NO_3 once again confirmed our conjecture *via* the FTIR analysis where plasticization helps in increment of NH_4NO_3 dissociation and with better diffusion rate; in turn it will produce more ions ready to hop to the COO^- group from the CMC–PVA backbone. Moreover, with an increased dissociation of NH_4NO_3 upon the addition of EC, the ions can easily hop from one site to another site and this phenomenon would influence the ionic conductivity of the plasticized system. Thus, plasticization has capability for the enhancement of ionic conductivity of SPEs which is confirmed by the increment of free ions by $\sim 30\%$ as compared to un-plasticized SPEs.

4. Conclusion

Biopolymer CMC blend with PVA doped with NH_4NO_3 plasticized PEG was successfully prepared by the solution casting method. Plasticization is able to enhance the dissociation of NH_4NO_3 . This plasticizing effect was confirmed by FTIR analysis where interaction *via* inter- and intra-H-bonding at the $-\text{OH}$ and COO^- of PEG and H^+ from NH_4NO_3 provides an alternative pathway for ion hopping within the SPEs. The formation of H-bonding promotes the miscibility among the constituents and reduces the T_g upon the addition of PEG. The SPEs with 8 wt% PEG shows the highest ionic conductivity which is $3.00 \times 10^{-3} \text{ S cm}^{-1}$ with the lowest activation energy of 0.026 eV. All SPE systems obey the Arrhenius characteristics within the studied temperature range. The number of mobile ions, ionic mobility and diffusion coefficient properties have confirmed that the mobile ions dominate in the ionic transport of the SPE system and has a correlation with the behaviour of ionic conductivity. Continued efforts are needed to further enhance the ionic conductivity of the SPEs including dual plasticization effect because the SPEs may be a good candidate for solid electrolyte system applications.

Acknowledgements

We would like to thank the Ministry of Higher Education (MOHE) for FRGS grant (RDU 1901114) and UMP Internal Grant (RDU 190389), Faculty Industrial Science and Technology, Universiti Malaysia Pahang for technical and research support.

References

- [1] Kim J G, Son B, Mukherjee S, Schuppert N, Bates A, Kwon O *et al* 2015 *J. Power Sources* **282** 299
- [2] Olivetti E, Gregory J and Kirchain R 2011 *Study conducted for the National Electric Manufacturers Association* (Cambridge, MA, USA: Massachusetts Institute of Technology)
- [3] Chen J 2013 *Materials* **6** 156
- [4] Whittingham M S 2004 *Chem. Rev.* **104** 4271
- [5] Shamsudin I, Ahmad A, Hassan N H and Kaddami H 2016 *Ionics* **22** 841
- [6] Solarajan A K, Murugadoss V and Angaiah S 2017 *J. Appl. Polym. Sci.* **134** 45177
- [7] Singh T J and Bhat S 2003 *Bull. Mater. Sci.* **26** 707
- [8] Parameswaran V, Nallamuthu N, Devendran P, Nagarajan E R and Manikandan A 2017 *Physica B* **515** 89
- [9] Aziz S B 2013 *Iran. Polym. J.* **22** 877
- [10] Mazuki N, Fuzlin A, Saadiah M and Samsudin A 2019 *Ionics* **25** 2657
- [11] Mazuki N F, Abdul Majeed A P P, Nagao Y and Samsudin A S 2020 *Polym. Test.* **81** 106234
- [12] Saadiah M and Samsudin A 2018 *AIP conference proceedings* p 020223
- [13] Gondaliya N, Kanchan D and Sharma P 2013 *Soc. Plast. Eng.* **10** 2417
- [14] Subramaniam R T, Chiam-Wen L, Yee L P and Morris E 2012 *Recent advances in plasticizers* (London, UK: IntechOpen) Chapter 9 p 165
- [15] Bhide A and Hariharan K 2007 *Eur. Polym. J.* **43** 4253
- [16] Woo H J, Majid S R and Arof A K 2013 *Solid State Ionics* **252** 102
- [17] Gupta S and Varshney P K 2017 *Ionics* **23** 1613
- [18] Kumar R, Sharma S, Pathak D, Dhiman N and Arora N 2017 *Solid State Ionics* **305** 57
- [19] Shin J, Jung S, Kim K, Ahn H and Ahn J 2002 *J. Mater. Sci.: Mater. Electron.* **13** 727
- [20] Ng L S and Mohamad A A 2006 *J. Power Sources* **163** 382
- [21] Chai M and Isa M 2016 *Sci. Rep.* **6** 27328
- [22] Zainuddin N and Samsudin A 2018 *Mater. Today Commun.* **14** 199
- [23] Arof A, Amirudin S, Yusof S and Noor I 2014 *Phys. Chem. Chem. Phys.* **16** 1856
- [24] Zainuddin N, Rasali N and Samsudin A 2018 *Ionics* **24** 3039
- [25] Rasali N and Samsudin A 2018 *Ionics* **24** 1639
- [26] Ramlli M, Maksud M and Isa M 2017 *AIP conference proceedings* p 020001
- [27] Sathiyarayanan P and Karunakaran R J 2015 *J. Chem. Pharm. Res.* **7** 1099
- [28] Karelin A I, Kayumov R R and Dobrovolsky Y A 2019 *Spectrochim. Acta Part A* **215** 381
- [29] Guo L, Sato H, Hashimoto T and Ozaki Y 2010 *Macromolecules* **43** 3897
- [30] Sharma P, Kanchan D, Gondaliya N, Pant M and Jayswal M S 2013 *Ionics* **19** 301
- [31] Deygen I M and Kudryashova E V 2016 *Colloids Surf. B* **141** 36
- [32] Samsudin A, Aziz M and Isa M 2012 *Int. J. Polym. Anal. Charact.* **17** 600
- [33] Jiang H, Zhang Q, Zhang Y, Sui L, Wu G, Yuan K *et al* 2019 *Phys. Chem. Chem. Phys.* **21** 10417
- [34] Hemalatha R, Alagar M, Selvasekarapandian S, Sundaresan B, Moniha V, Boopathi G *et al* 2019 *Ionics* **25** 141
- [35] Greco A, Ferrari F and Maffezzoli A 2018 *J. Therm. Anal. Calorim.* **134** 559
- [36] Ahmadi-Khaneghah A, Omidi-Ghallemohamadi M and Behniafar H 2019 *Int. J. Adhes. Adhes.* **95** 102430
- [37] Devangamath S S, Lobo B, Masti S P and Narasagoudr S 2020 *J. Mater. Sci.: Mater. Electron.* **31** 2904
- [38] Vieira M G A, da Silva M A, dos Santos L O and Beppu M M 2011 *Eur. Polym. J.* **47** 254
- [39] Aziz S B, Woo T J, Kadir M F Z and Ahmed H M 2018 *J. Sci. Adv. Mater. Dev.* **3** 1
- [40] Zhao L, Fu J, Du Z, Jia X, Qu Y, Yu F *et al* 2020 *J. Membr. Sci.* **593** 117428
- [41] Singh P, Bharati D C, Gupta P N and Saroj A L 2018 *J. Non-Cryst. Solids* **494** 21
- [42] Saadiah M A and Samsudin A S 2018 *IOP Conf. Ser.: Mater. Sci. Eng.* **342** 012045
- [43] Muhammad F H, Jamal A and Winie T 2017 *Ionics* **23** 3045
- [44] Hafiza M N and Isa M I N 2020 *J. Membr. Sci.* **597** 117176
- [45] Ambika C, Karuppasamy K, Vikraman D, Lee J Y, Regu T, Ajith Bosco Raj T *et al* 2018 *Solid State Ionics* **321** 106
- [46] Das S and Ghosh A 2015 *Electrochim. Acta* **171** 59
- [47] Dave G, Maheshwaran C and Kanchan D 2019 *AIP conference proceedings* p 030234
- [48] Samsudin A S and Saadiah M A 2018 *J. Non-Cryst. Solids* **497** 19
- [49] Ahmed H T, Jalal V J, Tahir D A, Mohamad A H and Abdullah O G 2019 *Results Phys.* **15** 102735
- [50] Selvalakshmi S, Mathavan T, Selvasekarapandian S and Premalatha M 2018 *Ionics* **24** 2209
- [51] Reddy C V S, Han X, Zhu Q-Y, Mai L-Q and Chen W 2006 *Eur. Polym. J.* **42** 3114
- [52] Selvasekarapandian S, Hema M, Kawamura J, Kamishima O and Baskaran R 2010 *J. Phys. Soc. Jpn.* **79** 163
- [53] Subban R H Y, Ahmad A, Kamarulzaman N and Ali A 2005 *Ionics* **11** 442
- [54] Balian S C, Ahmad A and Mohamed N 2016 *Polymers* **8** 163
- [55] Saadiah M A, Zhang D, Nagao Y, Muzakir S K and Samsudin A S 2019 *J. Non-Cryst. Solids* **511** 201
- [56] Rajendran S, Sivakumar M and Subadevi R 2003 *J. Power Sources* **124** 225
- [57] Ramesh S, Yahaya A and Arof A 2002 *Solid State Ionics* **152** 291
- [58] Rasali N, Nagao Y and Samsudin A 2019 *Ionics* **25** 641
- [59] Majid S and Arof A K 2005 *Physica B* **355** 78
- [60] Samsudin A and Isa M 2015 *Adv. Mater. Res.* **1108** 27
- [61] Noor N A M and Isa M I N 2019 *Int. J. Hydrog. Energy* **44** 8298
- [62] Ranjana P A B, Jeya S, Abarna S, Premalatha M, Arulsankar A and Sundaresan B 2019 *J. Polym. Res.* **26** 38